Received: 18 September 2021 | Revised: 18 March 2022 | Accepted: 20 March 2022

DOI: 10.1002/rcm.9301

RESEARCH ARTICLE

Rapid Communications in Mass Spectrometry WILEY

Temperature dependence of isotopic fractionation in the CO_2-O_2 isotope exchange reaction

Getachew Agmuas Adnew[1] | Evelyn Workman[1] | Christof Janssen[2] | Thomas Röckmann[1]

[1]Institute for Marine and Atmospheric Research Utrecht (IMAU), Physics Department, Utrecht University, Utrecht, The Netherlands

[2]Laboratoire d'Etudes du Rayonnement et de la Matière en Astrophysique et Atmosphères (LERMA), Sorbonne Université, Observatoire de Paris, Université PSL, Paris, France

Correspondence
G. A. Adnew, Institute for Marine and Atmospheric Research Utrecht (IMAU), Physics Department, Utrecht University, Princetonplein 5, Utrecht 3584CC, The Netherlands.
Email: g.a.adnew@uu.nl

Funding information
Wageningen University; Dutch Science Foundation NWO, Grant/Award Number: ALWPP.2016.013; EU Horizon 2020 ERC-ASICA, Grant/Award Number: 64908; Hebrew University of Jerusalem

Rationale: Oxygen isotope exchange between O_2 and CO_2 in the presence of heated platinum (Pt) is an established technique for determining the $\delta^{17}O$ value of CO_2. However, there is not yet a consensus on the associated fractionation factors at the steady state.

Methods: We determined experimentally the steady-state α^{17} and α^{18} fractionation factors for Pt-catalyzed CO_2-O_2 oxygen isotope exchange at temperatures ranging from 500 to 1200°C. For comparison, the theoretical α^{18} equilibrium exchange values reported by Richet et al. (1997) have been updated using the direct sum method for CO_2 and the corresponding α^{17} values were determined. Finally, we examined whether the steady-state fractionation factors depend on the isotopic composition of the reactants, by using CO_2 and O_2 differing in $\delta^{18}O$ value from −66 ‰ to +4 ‰.

Results: The experimentally determined steady-state fractionation factors α^{17} and α^{18} are lower than those obtained from the updated theoretical calculations (of CO_2-O_2 isotope exchange under equilibrium conditions) by 0.0024 ± 0.0001 and 0.0048 ± 0.0002, respectively. The offset is not due to scale incompatibilities between isotope measurements of O_2 and CO_2 nor to the neglect of non-Born-Oppenheimer effects in the calculations. There is a crossover temperature at which enrichment in the minor isotopes switches from CO_2 to O_2. The direct sum evaluation yields a θ value of ∼0.54, i.e. higher than the canonical range maximum for a mass-dependent fractionation process.

Conclusions: Updated theoretical values of α^{18} for equilibrium isotope exchange are lower than those derived from previous work by Richet et al. (1997). The direct sum evaluation for CO_2 yields θ values higher than the canonical range maximum for mass-dependent fractionation processes. This demonstrates the need to include anharmonic effects in the calculation and definition of mass-dependent fractionation processes for poly-atomic molecules. The discrepancy between the theory and the experimental α^{17} and α^{18} values may be due to thermal diffusion associated with the temperature gradient in the reactor.

1 | INTRODUCTION

Measurements of $\Delta'^{17}O$ (defined in Equation 1) of oxygen-containing molecules can provide insight into, for example, the carbon cycle and its link to the hydrological cycle[1–10] and are also used to reconstruct paleoclimate.[10–14] The $\Delta'^{17}O$ of CO_2 is a promising tracer to study the CO_2 exchange flux between the biosphere/hydrosphere and the atmosphere.[3,5,6,15] However, due to the mass interference of $^{13}C^{16}O^{16}O$ and $^{12}C^{17}O^{16}O$, it is difficult to measure $\delta^{17}O$ of CO_2 with existing isotope ratio mass spectrometers, because the required mass resolving power of about 55,000 (Δm/m) is a challenge for even the highest resolution instruments.[16] High precision and accuracy are needed for measurements of both $\delta^{18}O$ and $\delta^{17}O$ in order to capture the small, but non-zero deviations to use $\Delta'^{17}O$ as a tracer. Since the measurement of $\delta^{17}O$ directly from CO_2 with isotope ratio mass spectrometry (IRMS) is impossible due to the interference of $\delta^{13}C$, except from the fragment ions formed in the ion source,[16] indirect methods have been developed that enable the measurement of $\delta^{17}O$ of CO_2. These techniques are either based on isotope exchange or chemical conversion of CO_2 and are described in more detail in Adnew et al[16] and Hofmann and Pack.[17]

$$\Delta'^{17}O = \ln\left(\delta^{17}O + 1\right) - 0.528\ln\left(\delta^{18}O + 1\right) \quad (1)$$

The CO_2-O_2 exchange method was first developed by Mahata et al[18] and has been established in several laboratories, including our own.[11,12,16,19] Recently, the method has been extended to measure the $\Delta'^{17}O$ of water.[20] The CO_2-O_2 exchange method to measure $\Delta'^{17}O$ of CO_2 is less labor-intensive compared with other conversion/exchange methods and is capable of an impressive precision of < 0.01 ‰. Such precision allows the subtle seasonal $\Delta'^{17}O$ variability of tropospheric CO_2 to be quantified, with reported seasonal amplitudes between 0.02 ‰ and 0.13 ‰.[2,6,21]

The CO_2-O_2 exchange method is based on facilitating complete oxygen isotope exchange between CO_2 and O_2 at high temperature in the presence of a platinum catalyst. This way, the oxygen isotopic composition of the CO_2 is imprinted on O_2 and the ^{17}O content of the CO_2 sample can be calculated from measurement of the isotopic composition of O_2 before and after the isotope exchange. Important parameters in the calculation of the $\Delta'^{17}O$ of CO_2 are the molar ratio of CO_2 and O_2 and the isotopic fractionation factors (α).

$$\alpha^I(CO_2/O_2) = \frac{\left({}^I R_f\right)_{CO_2}}{\left({}^I R_f\right)_{O_2}} = \frac{\left(\delta^I O_f + 1\right)_{CO_2}}{\left(\delta^I O_f + 1\right)_{O_2}} \quad (2)$$

The index I is a placeholder for either 17 or 18. The fractionation factors $\alpha^{17}(CO_2/O_2)$ and $\alpha^{18}(CO_2/O_2)$ determine the distribution of the heavy isotopes between O_2 and CO_2 at isotopic steady state.

The CO_2-O_2 exchange technique has been used in different laboratories to study the carbon cycle[1–4,6,22,23] and precise measurement of $\Delta'^{17}O$ is used to correct for biases in clumped isotope measurements of CO_2.[24–27] However, the fractionation factor in CO_2-O_2 isotope exchange is not well established, and different values have been reported by different laboratories.

One explanation for these differences may be variations in the effective isotope exchange temperature, as the fractionation factor is expected to be temperature dependent. Furthermore, the mechanism of the CO_2-O_2 isotope exchange in the presence of a platinum catalyst is unknown.[16,18,19,26,28,29] In this study we determined $\alpha^{17}(CO_2/O_2)$ and $\alpha^{18}(CO_2/O_2)$ for the CO_2-O_2 exchange method over a temperature range from 500°C to 1200°C. We investigated whether there is a dependency on the initial oxygen isotopic composition of CO_2 and O_2. This also addresses a potential effect of an isotope scale difference between CO_2 and O_2. We revisit and update theoretical calculations of the isotope equilibrium by Richet et al. (1997)[30] and calculated the three-isotope exponent (θ) of the CO_2-O_2 equilibrium isotope exchange for a temperature range of 0°C to 1200°C.

2 | MATERIALS AND METHODS

2.1 | Theoretical calculations of CO_2-O_2 isotope exchange at equilibrium

Fractionation factors ${}^{17}\alpha$ and ${}^{18}\alpha$ for the CO_2-O_2 isotope exchange can be calculated from statistically corrected equilibrium constants of O-atom exchange reactions with CO_2 and O_2, respectively. The latter are conveniently designated as β-factors and were originally introduced as fractionation factors between the fully substituted molecule and O-atom (${}^I\beta_A = ([{}^I O]/[{}^{16}O])_A/([{}^I O]/[{}^{16}O])_{Atomic-O}$, where A is either CO_2 or O_2).[30–33] Since in the measurements of the equilibrium constants multi-substituted species have been neglected, we define quantities α and β slightly differently:

$$\alpha^I = \frac{Q\left(C^{16}O^I O\right)}{Q\left(C^{16}O_2\right)}\frac{Q\left({}^{16}O_2\right)}{Q\left({}^{16}O^I O\right)} = \frac{Q\left(C^{16}O^I O\right)Q\left({}^{16}O\right)}{Q\left(C^{16}O_2\right)Q\left({}^I O\right)} \Big/ \frac{Q\left({}^{16}O^I O\right)Q\left({}^{16}O\right)}{Q\left({}^{16}O_2\right)Q\left({}^I O\right)} = \frac{{}^I\beta_{CO_2}}{{}^I\beta_{O_2}}, \quad (3)$$

where Q are the total partition functions. For the calculation of these exchange equilibria, molecular partition functions were divided into internal and translational parts. Total internal partition functions and ratios of diatomic molecules were calculated using the formalism of Urey[34] and Bigeleisen and Mayer,[35] including anharmonic corrections and zero-point energy expressions based on Dunham's[36] expression of energy levels (see Richet et al. (1997)[30]). Molecular constants of the $^{16}O_2$ species were taken from Huber and Herzberg[37] in combination with recent atomic masses[38] and those of the isotopic variants were calculated using the standard mass dependence of Dunham coefficients. This choice of molecular constants is compatible with a recent recommendation[39] and an agreement to

better than five significant digits is obtained across the temperature range. However, our current results are slightly different from a previously published parametrization[40] – the less than 0.2 ‰ difference being mainly due to the identification and removal of an error in the calculation of a correction term.

Unfortunately, application of Dunham's approach to larger molecules is not straightforward, because the isotope scaling of anharmonic vibrational constants is neither theoretically well constrained nor experimentally known, and the constant zero-point energy offset G_0 is not known either.[30] We have therefore calculated the total internal partition functions of the ^{16}O-, ^{17}O-, and ^{18}O-containing isotopologues of $^{l}O^{12}C^{16}O$ as direct sums of overall energy levels obtained from the spectroscopically adjusted ab-initio line list calculations of Huang et al[41,42] (see Prokhorov et al[43] for more details).

Our new calculations were verified by comparing atom-diatom isotope exchange equilibria (β-values) with the tables of Richet et al. (1997)[30] using several isotopes and diatomic molecules (^{13}C exchange in CO and CS, ^{15}N exchange in N_2, and ^{18}O exchange in CO and O_2). These results agreed across the temperature range between 0°C and 1200°C, to better than 0.7 ‰ for all molecules except for O_2, where our values were higher by 4 ‰ at 0°C and 1 ‰ at 1200°C (see Table S1, supporting information). We have discovered a subtle difference in the molecular constants used in this study and that of Richet et al. (1997)[30] but such slight differences cannot account for the observed discrepancy. Interestingly, Richet et al. (1997)[30] report the same 4 ‰ discrepancy when comparing their 25°C results with the calculations of Urey[32] (see Table 16 in Richet et al. (1997)[30]), while the β-values for O-, C-, or N-exchange with other diatomic molecules always agree with the work of Urey to within 1 ‰. It needs be pointed out that the discrepancy is not due to our slightly different definition of β and our neglect of excess factors, since it even increases if we calculate β-values from doubly substituted O_2. This indicates that an error must have occurred in the O_2 calculations of Richet et al. (1997).[30]

When comparing our atom-CO_2 exchange equilibria with Richet et al. (1997)[30] the agreement is better, but still worse compared with diatomic gases when O_2 is excluded from the comparison. For the ^{18}O exchange, our β-values are 2 ‰ higher at 0°C and less than 1 ‰ for relevant temperatures above 400°C (see supporting information). For ^{13}C exchange, our values at 0°C are 1.3 ‰ higher and the discrepancy becomes already smaller than 1 ‰ at temperatures above 100°C.

The comparison of $\alpha^{18}(CO_2/O_2)$ between our calculation and that of Richet et al. (1997)[30] for the temperature range between 0°C and 1200°C is also shown in Table S2 (supporting information). Our $\alpha^{18}(CO_2/O_2)$ value agrees with that reported by Richet et al. (1997)[30] to within 1 ‰, for temperatures higher than 450°C. However, at low temperature the difference is higher than 1 ‰ (for instance 2.2 ‰ at 0°C; see Table S2, supporting information). This is because our β-factors for both O_2 and CO_2 are different from the values reported by Richet et al. (1997)[30] the difference being largest in O_2, where we suspect the calculation of Richet et al. (1997)[30] is erroneous (see Table S1, supporting information).

We have compared partition function ratios $Q(^{13}CO_2)/Q(^{12}CO_2)$ of ^{16}O- and ^{18}O-containing isotopologues also with results from path integral Monte Carlo calculations of Webb and Miller[44] over the 300 to 600 K range and found deviations of less than 0.5 ‰ and 0.3 ‰ at 300 K and 600 K, respectively. This confirms that CO_2-related uncertainties of $^{18}\alpha$ should be smaller than 0.3 ‰ for most of the temperatures in this study. Higher electronic states of both molecules have been neglected in the calculations. At transition energies of 5.7 eV ($1^1A_1''$ CO_2[45]) and 0.98 eV ($a^1\Delta_g$ O_2[37]), the population of electronically excited CO_2 is completely negligible and the $O_2(^1\Delta)$ ground state is only marginally populated (by less than 8 parts in 10^5), even at the highest temperature. The effect on isotope ratios is much smaller because geometric changes in excited oxygen isotopes are small, and vibrational and rotational constants of the excited state are similar to the ground state values (changing by 7 % at most).[37]

2.2 | CO_2-O_2 exchange system

A detailed description of the CO_2-O_2 exchange method established at Utrecht University is given elsewhere.[1,16] In brief, equal amounts of CO_2 and O_2 were allowed to equilibrate in a quartz reactor in the presence of platinum sponge as a catalyst (purity ≥ 99.9 %, Sigma Aldrich, USA) at the bottom of the reactor. The CO_2-O_2 exchange experiments were performed at temperatures between 500 and 1200°C. The temporal evolution of the isotope exchange was determined at 650°C, 750°C, and 850°C by varying the duration of the CO_2-O_2 exchange. After the exchange reaction, CO_2 and O_2 were separated cryogenically and the O_2 collected at liquid nitrogen temperature on molecular sieve 5 Å pellets (3 pellets, 5 mm long, 1.8 mm o.d., Sigma Aldrich, USA). The isotope measurements were performed on a Delta V Plus isotope ratio mass spectrometer (Thermo Scientific, Germany) in dual inlet mode. A schematic of the exchange reactor is shown in Figure 1. For comparison, the reactor that was used in Adnew et al. (2019)[16] is shown in Figure S1 (supporting information). The main difference between the current setup and the one used in the previous study[16] is an electropolished stainless steel extension.

2.3 | Samples

Three commercial O_2 gases with different isotope compositions were used for the measurements (Table 1). The working reference gas (GO_2-1) has $\delta^{17}O = 9.235 \pm 0.011$ ‰ and $\delta^{18}O = 18.514 \pm 0.011$ ‰ (Table 1), determined by Eugeni Barkan, Hebrew University of Jerusalem. For CO_2 we used two gases from high-pressure cylinders (GCO_2-3 and GCO_2-4) and two additional gases (GCO_2-1 and GCO_2-2) that were prepared by combusting a graphite rod with two isotopically different O_2 gases[16,46–49] (GO_2-1 and GO_2-2,

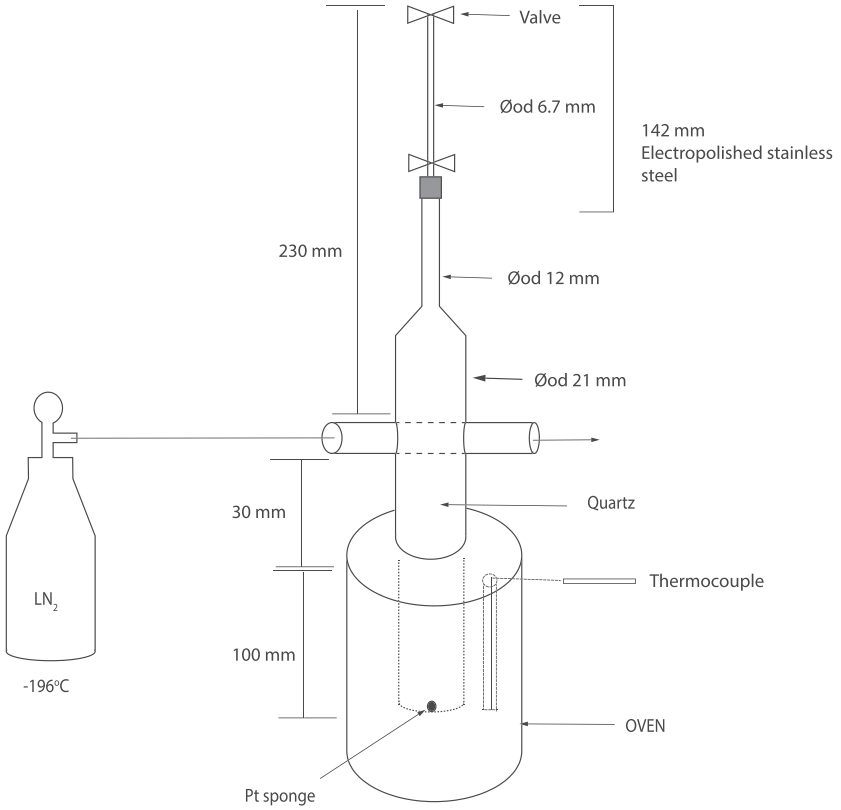

FIGURE 1 Geometry and dimensions of the CO_2-O_2 reactor

TABLE 1 Overview of names, suppliers, and isotopic compositions of the CO_2 and O_2 working standards used in this study. All the CO_2 gases used had a purity of > 99.995 % except for the ones that were produced in the laboratory by combustion of a graphite rod. O_2 gases had a purity of > 99.998 %. All isotopic values are given in ‰, relative to VPDB for $\delta^{13}C$ and relative to VSMOW for $\delta^{17}O$ and $\delta^{18}O$. The errors are reported as one standard deviation (σ)

CO_2 gases used in this study				
Name	**Source/supplier**	**$\delta^{13}C$**	**$\delta^{18}O$**	**$\Delta'^{17}O$**
GCO_2-1	Combustion	−26.160 ± 0.030	17.921 ± 0.042	−0.465 ± 0.018
GCO_2-2	Combustion	−26.154 ± 0.059	−38.205 ± 0.051	−0.518 ± 0.016
GCO_2-3	Linde Gas, The Netherlands	−31.665 ± 0.005	34.655 ± 0.011	−0.242 ± 0.003
GCO_2-4	Air Products, Germany	−10.332 ± 0.005	30.082 ± 0.011	−0.169 ± 0.002
O_2 gases used in this study				
Name	**Source/supplier**	**$\delta^{17}O$**	**$\delta^{18}O$**	**$\Delta'^{17}O$**
GO_2-1	Air Products, The Netherlands	9.235 ± 0.011	18.514 ± 0.011	−0.494 ± 0.011
GO_2-2	Air Liquide, The Netherlands	−20.734 ± 0.017	−37.862 ± 0.012	−0.573 ± 0.017
GO_2-3	Linde Gas, The Netherlands	7.040 ± 0.021	14.095 ± 0.011	−0.375 ± 0.020

respectively). The isotopic compositions of the CO_2 and O_2 used in this study are shown in Table 1. The experimental procedure for the combustion experiment is described in detail elsewhere.[16] In summary, the graphite rod (99.9995% purity, 3.05 mm × 20 mm, Alfa Aesar, Part No: 40765, Thermo Fisher Scientific) was wrapped in a sheet of platinum foil and platinum wire and placed inside a quartz reactor. The combustion with O_2 was performed at 800°C. Before starting the experiment, the graphite rod was cleaned for more than 24 h by heating at 1000°C in high vacuum. After each conversion experiment, the graphite rod was again cleaned by heating at 1000°C for at least 1 h.

3 | RESULTS

The differences in isotopic composition of the two working standards (GCO_2-3 and GCO_2-4) are 4.440 ± 0.015 ‰ for $\delta^{18}O$ and −21.556 ± 0.007 ‰ for $\delta^{13}C$. respectively (Table 1). In our laboratory, we measured relative differences of 4.479 ± 0.003 ‰ for $\delta^{18}O$ and −21.448 ± 0.001 ‰ for $\delta^{13}C$, respectively, from six replicates. For each measurement new gas was introduced to the bellows. Similarly, for GO_2-1 and GO_2-2, the relative difference was −29.690 (−29.746) ‰ for $\delta^{17}O$ and −55.456 (−55.432) ‰ for $\delta^{18}O$, respectively. The values in parentheses are the assigned differences based on the

measurements at Hebrew University (E. Barkan). Overall, the assigned and measured values agree well.

3.1 | CO_2-O_2 isotope steady state

Figure 2 shows the temporal evolution of the CO_2-O_2 isotope exchange for temperatures of 650°C, 750°C, and 850°C. The exchange proceeds faster at higher temperatures, as expected.

The data sets at each of the three reaction temperatures are fitted to an exponential curve of the form $y = A + B \times e^{-k \times t}$, where y is the isotopic composition ($\delta^{17}O$ or $\delta^{18}O$) of O_2 at time t, A is the isotopic composition at long time scales (Figure 2), $A + B$ is the isotopic composition of O_2 at $t = 0$, k is the rate constant of the reaction, and t is the reaction time. In our experiments we defined steady state as having been achieved when k determined from the fit for each temperature $e^{-kt} < 10^{-6}$, i.e. $t = 13.816/k$. From these fits, the respective steady state values of $\delta^{17}O_f$ and $\delta^{18}O_f$ of the O_2 are 2.684 ‰ and 5.032 ‰ at 650°C; 3.018 ‰ and 5.648 ‰ at 750°C; and 3.278 ‰ and 6.100 ‰ at 850°C. The enrichments of ^{17}O and ^{18}O in the O_2 at steady state increase with reaction temperature (Figures 2 and 3A).

Figure 3A shows the steady state isotopic composition $\delta^{18}O_f$ (O_2) and $\delta^{18}O_f$ (CO_2) for reaction temperatures ranging from 500 to 1200°C. In Figure 3B the fractionation factors $\alpha^{17}(CO_2/O_2)$ and $\alpha^{18}(CO_2/O_2)$ derived from these steady state enrichments are shown. As can be seen, α^{17} and α^{18} decrease with increasing reaction temperature. The exchange reactions were carried out using gases GCO_2-4 ($\delta^{18}O = 30.082$ ‰) and GO_2-3 ($\delta^{18}O = 14.095$ ‰), see Table 1. Figure 3 shows that below 810°C, $\delta^{18}O_f$ (CO_2) > $\delta^{18}O_f$ (O_2) and $\alpha^{18}(CO_2/O_2) > 1$; thus there is a slight preference for the CO_2 to be relatively enriched in ^{17}O and ^{18}O. At higher temperatures, this preference is reversed, with $\alpha^{18} < 1$, i.e. $\delta^{18}O_f$ (CO_2) < $\delta^{18}O_f$ (O_2).

3.2 | Dependence of $\alpha^{17}(CO_2/O_2)$ and $\alpha^{18}(CO_2/O_2)$ on the relative difference between the initial oxygen isotopic compositions of CO_2 and O_2

The isotopic steady state should be a property of the reaction system and independent of the isotopic composition of the initial reagents. To confirm this, we used O_2 and CO_2 with a wide range of isotopic compositions, with a $\delta^{18}O$ difference of the initial O_2 and CO_2 by up to −65.96 ‰ in exchange experiments at 650°C, 750°C, and 850°C.

Figure 4 demonstrates that the same values for $\alpha^{17}(CO_2/O_2)$ and $\alpha^{18}(CO_2/O_2)$ are reached in experiments where the isotopic composition of the starting gases is very different, confirming that $\alpha^{17}(CO_2/O_2)$ and $\alpha^{18}(CO_2/O_2)$ values are independent of the initial isotopic composition of CO_2 and O_2.

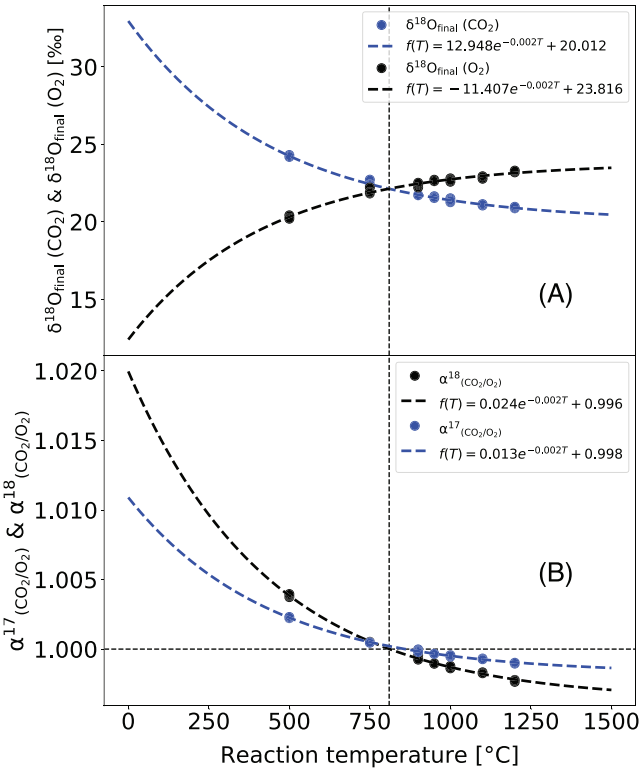

FIGURE 3 A, $\delta^{18}O(O_2)$ and $\delta^{18}O(CO_2)$ after CO_2-O_2 exchange at isotope exchange steady state for reaction temperatures ranging from 500°C to 1200°C. B, The corresponding fractionation factors $\alpha^{17}(CO_2/O_2)$ and $\alpha^{18}(CO_2/O_2)$. The vertical dashed line shows the temperature at which $\alpha^{17}(CO_2/O_2)$ and $\alpha^{18}(CO_2/O_2)$ cross the value of 1 (horizontal dashed line). In the fit function, T is the temperature in °C [Color figure can be viewed at wileyonlinelibrary.com]

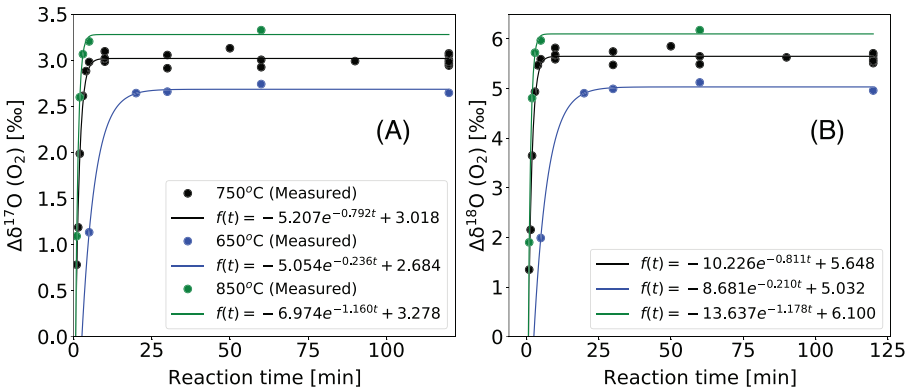

FIGURE 2 Temporal evolution of $\delta^{17}O$ (O_2) (A) and $\delta^{18}O$ (O_2) (B) during CO_2-O_2 exchange on a platinum sponge catalyst in a quartz reactor, for reaction temperatures of 650°C, 750°C, and 850°C. $\Delta\delta^{17}O(O_2)$ and $\Delta\delta^{18}O$ (O_2) are the differences in $\delta^{17}O$ and $\delta^{18}O$, respectively, between the initial and final isotopic compositions of O_2 [Color figure can be viewed at wileyonlinelibrary.com]

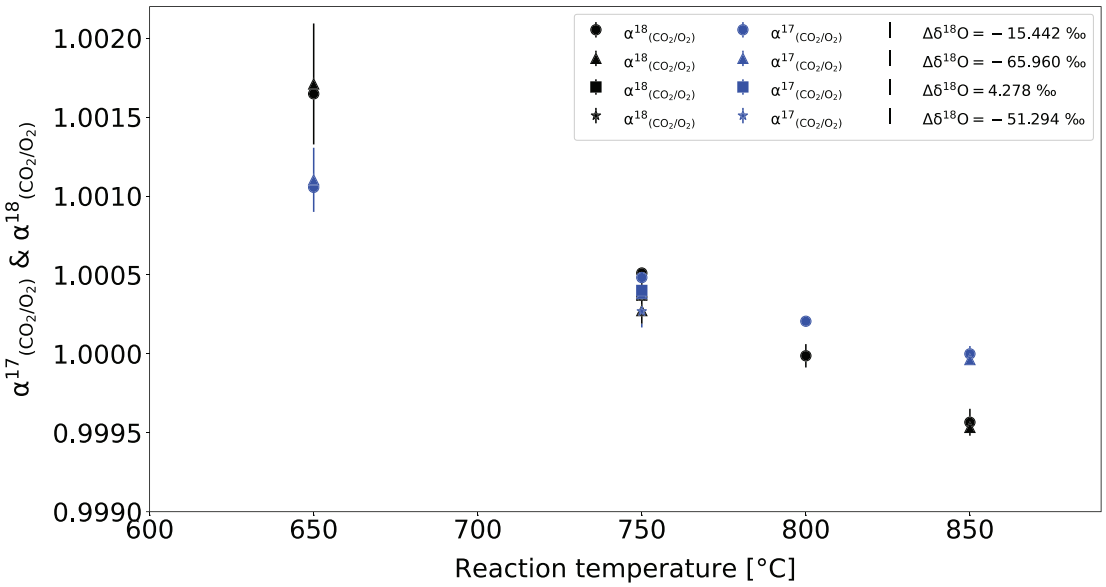

FIGURE 4 Dependence of $\alpha^{17}(CO_2/O_2)$ (blue symbols) and $\alpha^{18}(CO_2/O_2)$ (black symbols) on the initial isotopic composition of CO_2 and O_2 (see legend for the relative difference in $\delta^{18}O$ between CO_2 and O_2). The rectangle and star symbols are for CO_2 samples produced by the combustion of a graphite rod with O_2. $\Delta\delta^{18}O$ is the initial $\delta^{18}O$ difference between CO_2 and O_2 [Color figure can be viewed at wileyonlinelibrary.com]

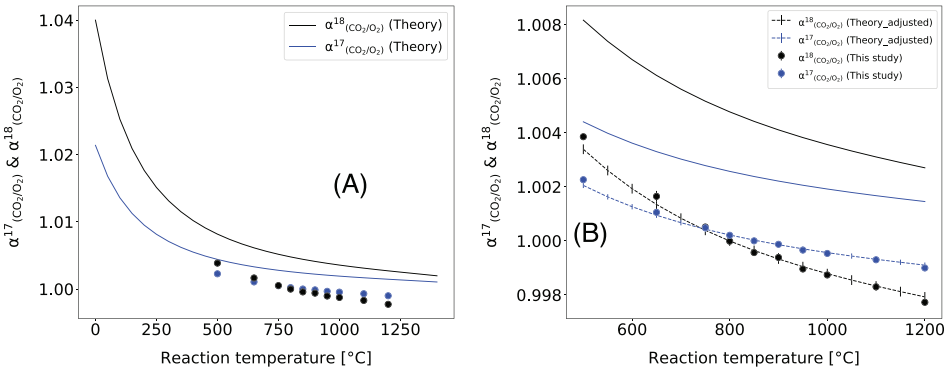

FIGURE 5 A, Dependence of measured $\alpha^{17}(CO_2/O_2)$ and $\alpha^{18}(CO_2/O_2)$ on temperature, together with data from theoretical equilibrium calculations. In B) the temperature scale has been adjusted to that of the experiments and the theoretically derived equilibrium values for $\alpha^{17}(CO_2/O_2)$ and $\alpha^{18}(CO_2/O_2)$ (solid lines) have been corrected for the respective mean offsets in $\alpha^{17}(CO_2/O_2)$ and $\alpha^{18}(CO_2/O_2)$ (dashed lines) [Color figure can be viewed at wileyonlinelibrary.com]

3.3 | Comparison with theoretical calculations

Figure 5A shows that $\alpha^{17}(CO_2/O_2)$ and $\alpha^{18}(CO_2/O_2)$ depend on temperature. This holds for both the experimental steady state results and the theoretically calculated thermodynamic equilibrium values, with the shapes of the temperature dependence being similar between theory and experiment. Interestingly, the calculated results are higher than the experimental data. As shown in Figure 6, the offset between the experimental values and theoretical equilibrium calculation is not constant but has a slight temperature dependence.

The average offset between the theoretically calculated and the experimental values is 0.0024 ± 0.001 and 0.0048 ± 0.002 for $\alpha^{17}(CO_2/O_2)$ and $\alpha^{18}(CO_2/O_2)$, respectively. This offset is very close to mass-dependent fractionation with a triple oxygen isotope fractionation (θ) value of 0.5. For the CO_2-O_2 exchange experiment, θ is calculated as shown in Equation 4.

$$\theta(CO_2/O_2) = \frac{\ln(\alpha^{17}(CO_2/O_2))}{\ln(\alpha^{18}(CO_2/O_2))} \quad (4)$$

In Figure 5B we have shifted the theoretical $\alpha^{17}(CO_2/O_2)$ and $\alpha^{18}(CO_2/O_2)$ by the average offset from the experimental value, which results in a very good agreement with the experimentally determined values. The difference between the theoretical and measured $\alpha^{17}(CO_2/O_2)$ and $\alpha^{18}(CO_2/O_2)$ values show a slight increase with temperature (Figure 6). This trend diminishes at temperatures above 800°C.

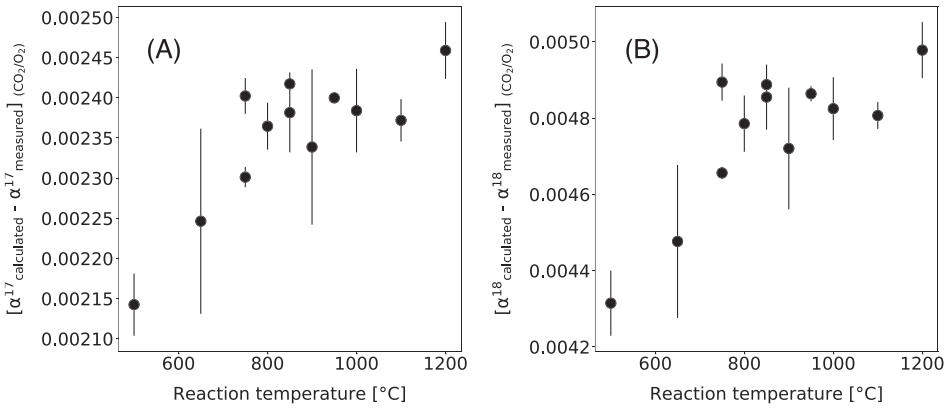

FIGURE 6 Temperature dependence of the experimental $\alpha^{17}(CO_2/O_2)$ and $\alpha^{18}(CO_2/O_2)$ offsets from the theoretical equilibrium values

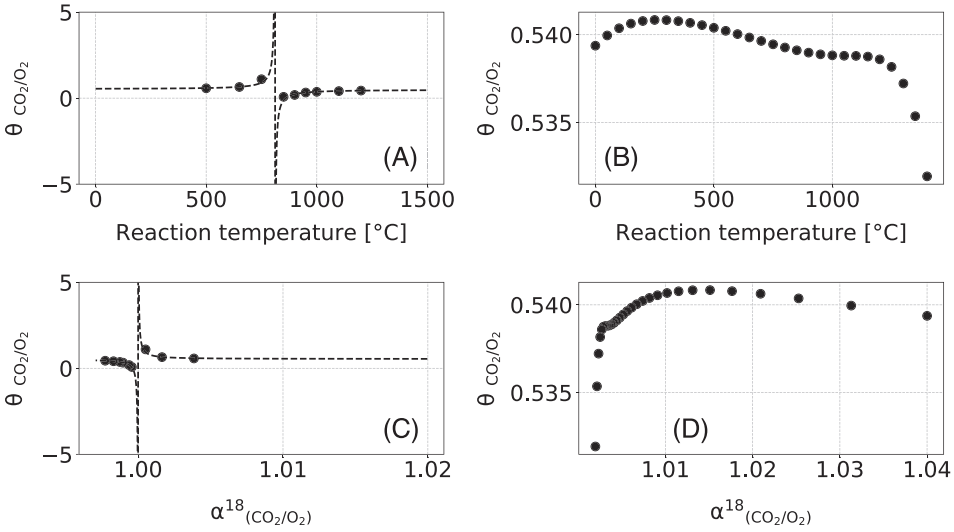

FIGURE 7 Dependence of θ (CO_2/O_2) on reaction temperature and $\alpha^{18}(CO_2/O_2)$ value for experimental data (A and C) and theoretical calculation (B and D). In (A) and (C), the dashed line is the θ (CO_2/O_2) value calculated from the fit function of Figure 3: $\alpha^{18}(CO_2/O_2) = 0.024\ \exp(-0.002\ T) + 0.996$; $\alpha^{17}(CO_2/O_2) = 0.013\exp(-0.002\ T) + 0.998$

According to the theoretical calculations, the fractionation at higher temperatures should approach unity. However, as mentioned above, experimentally we observe a fractionation of less than unity at higher temperatures, where the $\delta^{18}O$ of the exchanged O_2 is higher than the $\delta^{18}O$ of CO_2 (Figures 3 and 4).

3.3.1 | Scale difference between O_2 and CO_2

To check if the discrepancy of $\alpha^{17}(CO_2/O_2)$ and $\alpha^{18}(CO_2/O_2)$ between the experimental results and theoretical equilibrium estimates is due to the scale difference between the CO_2 and O_2, we used CO_2 formed from combustion of a graphite rod as described in section 2.3. The difference in $\delta^{18}O$ between GO_2-3 and GO_2-1 was −55.335 ‰. After combustion of the graphite rod with both GO_2-1 and GO_2-2, the relative difference between the produced GCO_2-1 and GCO_2-2 was −55.169 ‰. A potential scale difference is thus of the order 0.2 ‰, but these small differences between $\delta^{18}O$ of the oxygen used for combustion and the $\delta^{18}O$ of the resulting CO_2 might also be due to incomplete combustion and/or CO formation.[16,46–49] After assessing the potential scale discrepancies, we performed the same equilibration experiments with these gases at a reaction temperature of 750°C. As shown in Figure 4, the discrepancy between the theoretically estimated equilibrium fractionation in $\delta^{17}O$ and $\delta^{18}O$, and the experimental results after isotopic exchange between CO_2 and O_2 at steady state, is similar for all combinations of CO_2 and O_2, including the gases where scale discrepancies were specifically assessed. This provides evidence that the offset is not due to scale differences between the O_2 and CO_2 isotope scales.

3.4 | Dependence of θ (CO_2/O_2) on CO_2-O_2 equilibration temperature

As shown in Figure 7, θ (CO_2/O_2) is dependent on the CO_2-O_2 equilibration temperature. θ (CO_2/O_2) takes on extreme values close to the crossover (−∞ to ∞). In addition, for α values close to 1, small experimental errors will lead to large variability in θ (CO_2/O_2). The theoretical calculation does not show any crossover temperature, unlike the experimental values. Due to the crossover in the experiments between 750 and 800°C, θ values are largely outside the canonical range between 0.5 and 0.5305.[31,50–53] In contrast, the calculated θ (CO_2/O_2) value systematically exceeds the canonical upper limit $\theta_{HTL} = 0.5305$ and remains close to 0.54 across the

temperature range between 0°C and 1200°C. We suspect that the drop in θ (CO_2/O_2) at temperatures >1250°C in Figure 7 is an artefact, likely to be due to not including some high-energy states in the calculations.[43,54,55] This concerns mostly the rarest (^{17}O containing) isotopologue, on which the least experimental information is available.

4 | DISCUSSION

4.1 | Reaction rate constant of the CO_2-O_2 isotope exchange reaction

The rate for the CO_2-O_2 isotope exchange reaction in the presence of a platinum catalyst depends on the exchange temperature. As shown in Figure 2, isotope steady state between CO_2 and O_2 was reached in less than 1 h at reaction temperatures of 650°C, 750°C, and 850°C. However, at 500°C, the results indicated that the isotopic steady state was not reached within 2 h ($\alpha^{17}(CO_2/O_2) = 1.0010$ and $\alpha^{18}(CO_2/O_2) = 1.0187$), see Table S3 (supporting information). Mahata and co-authors[28] reported an increase in the $\delta^{18}O$ value of oxygen with temperature which they attributed to an enhancement in the catalytic activity of the platinum. Our data on the temperature dependence of $\alpha^{18}(CO_2/O_2)$ show (after accounting for an offset, discussed later) very good agreement with the theoretical equilibrium calculations over the entire temperature range of 500 to 1200°C. This demonstrates that the increase in the $\delta^{18}O$ value of the oxygen is not due to the efficiency of the catalyst but reflects the thermodynamically expected behavior. However, we did observe a decrease in the efficiency of the platinum sponge catalyst after it was exposed to a higher temperature. For example, after exposure to 1200°C, it took a long time to reach isotopic steady state at a lower temperature (e.g. at 650°C), which most likely indicates some kind of sintering of the platinum sponge, leading to a reduction in active surfaces and thus a decrease in catalytic efficiency. The efficiency of the catalyst only affects the duration required to attain CO_2-O_2 isotope exchange, not the final isotopic composition.

4.2 | $\alpha^{17}(CO_2/O_2)$ and $\alpha^{18}(CO_2/O_2)$ of the CO_2-O_2 isotope exchange reaction

As described in section 3.3, the experimental values for $\alpha^{17}(CO_2/O_2)$ and $\alpha^{18}(CO_2/O_2)$ are lower than the corresponding theoretical equilibrium estimates, and they cross from values above 1 to values below 1 at higher temperatures, in contrast to the theoretical equilibrium calculations. One shortcoming of the current work is that the calculations of α values involve the assumption of the Born-Oppenheimer approximation in the analysis of spectral data leading to the partition functions in Equation 2. However, this assumption is only approximate and it is possible that neglecting these effects could at least partly explain the difference between experiment and theory. Based on the work of Born and Huang,[56] Zhang and Liu[57] give an expression for the correction of a partition function ratio for a heavy and light isotope pair, which essentially implies that there is an additional constant shift (ΔE) in the energy levels between the heavy and the light molecules of an isotope pair, leading to an additional term $\exp(-\Delta E/k_B T)$ in the calculation of the partition function ratios and the equilibrium constant (where k_B is Boltzmann's constant). These effects are strongly temperature dependent and vanish at high temperatures. Such behavior is not compatible with our observation of a temperature-independent offset and we consequently exclude the notation non-Born-Oppenheimer effects could explain the observed discrepancy.

Mahata and co-authors[18] also reported $\alpha^{18}(CO_2/O_2) < 1$, ranging from 0.998128 to 0.99463, even at 680°C. Table 2 shows that all recently published $\alpha^{17}(CO_2/O_2)$ and $\alpha^{18}(CO_2/O_2)$ values are lower compared with the theoretically calculated equilibrium value for

TABLE 2 Theoretically calculated equilibrium values (this study) and experimentally determined values of $\alpha^{17}(CO_2/O_2)$ and $\alpha^{18}(CO_2/O_2)$ from this study (*) and from recent publications. All the experimentally determined values are lower than the theoretically calculated equilibrium ones

	Theoretical values (this study)		Experimental values			
Temp. [°C]	$\alpha^{17}(CO_2/O_2)$	$\alpha^{18}(CO_2/O_2)$	$\alpha^{17}(CO_2/O_2)$	$\alpha^{18}(CO_2/O_2)$	θ (CO_2/O_2)	Ref.
600	1.0036	1.0067	-	1.0031–1.00785		30
670	1.0032	1.0059	0.99977	0.9990	0.229911	29
680	1.0031	1.0058	-	0.998 to 0.995		19
700	1.0030	1.0056	-	0.9997–1.00414		30
750	1.0028	1.0052	1.00135	1.00227	0.594987	20
			1.00125	1.00215	0.581657	12
			1.00082	1.00141	0.581732	13
			1.000666	1.000998	0.667445	17
			1.00048	1.00051	0.941191	*
800	1.0026	1.0048	-	0.9998–1.001269		30
			0.9990	0.9977	0.4345	28
			1.0002065	0.999988	−17.2065	*

CO_2-O_2 exchange temperatures of 600°C to 800°C. The presence of the platinum sponge, the geometry of the experimental setups, and the temperature gradient between the cold and hot zones of the reactor were postulated as possible sources of the discrepancy between the measured fractionation value and the theoretically estimated thermodynamic equilibrium value.

Based on the results of the O_2-CO_2 conversion experiments, the discrepancy between the experimental and theoretically calculated equilibrium values of $\alpha^{18}(CO_2/O_2)$ and $\alpha^{17}(CO_2/O_2)$ is not due to an isotopic scale difference between O_2 and CO_2. In addition, $\alpha^{18}(CO_2/O_2)$ and $\alpha^{17}(CO_2/O_2)$ values are independent of the initial oxygen isotope composition of the CO_2 and O_2 and also do not depend on the relative difference in the oxygen isotope composition between the initial CO_2 and O_2. Thus, the discrepancy must have other causes.

Oxygen isotope exchange between CO_2 or O_2 and the quartz reactor tube has been shown to be negligible in our experiments at 750°C.[16,19] We did not investigate whether it occurs at higher temperatures, but Barkan and Luz[46] reported that isotope exchange between oxygen and quartz at temperatures of up to 950°C is negligible. Similarly, Saeger et al[26] reported no significant exchange between quartz and O_2 nor between quartz and CO_2 at 800°C. The effect of oxygen isotope exchange with quartz will be higher if the $\delta^{18}O$ value of the quartz is very different from that of the CO_2 or O_2. Quartz glass tubing is mostly made from silica sand having $\delta^{18}O$ values ranging from 10 ‰ to 20 ‰,[58] which is relatively close to the $\delta^{18}O$ value of the O_2 used for characterizing the CO_2-O_2 exchange reaction in this study (GO_2-3). The potential for isotope exchange should depend on the relative difference in oxygen isotopic composition between the quartz, CO_2, and O_2. However, even if there is isotope exchange with quartz, it only affects the $\delta^{17}O$ and $\delta^{18}O$ values of CO_2 and O_2 after exchange, not the $\alpha^{17}(CO_2/O_2)$ and $\alpha^{18}(CO_2/O_2)$ values.

A possible explanation for the discrepancy between the calculation and the experimental results is isotopic separation due to thermal diffusion.[59–64] In this study, one end of the reactor is positioned inside an oven at a specific temperature (500°C to 1200°C), whereas the other end is at room temperature (see Figure 1). The hot zone of the reactor is only 35 cm^3 in volume and approximately half that is outside the oven (Figure 1). Due to thermal diffusion, the heavier isotopes will accumulate in the cold zone of the reactor compared to the hot zone.[59–61,65,66] The relative separation of the isotopologues is proportional to their mass difference. The thermal diffusion factor of the heavy isotopologue relative to the light isotopologue is $(\alpha_{21}) = \alpha_o(m_2 - m_1)/(m_1 + m_2)$ where m_1 and m_2 are the molecular masses of the light and heavy isotopologues, respectively, and α_o is the reduced thermal diffusion factor which depends only on temperature and the intermolecular force between isotopes.[60,67] A detailed description of thermal diffusion and the thermal diffusion factor is presented in the literature[60,67] and references cited therein. The isotope separation between the cold and hot zones for O_2 isotopologues is higher than for CO_2 isotopologues.[60,65] Thus, the O_2 in the cold zone of the reactor will be more enriched in heavy isotopes compared with CO_2, resulting in $\alpha^{17}(CO_2/O_2)$ and $\alpha^{18}(CO_2/O_2)$ being lower than as calculated for thermodynamic equilibrium.

The effect of thermal diffusion should depend on the geometry and the temperature gradient between the cold and hot zones of the reactor. Horizontally oriented reactors are less convective and could result in larger isotope fractionation compared to a vertically oriented reactor. Mahata and co-authors[28] used a horizontal reactor, and in fact the results from their study show a higher discrepancy with respect to the theoretical calculations (3.4 ‰ and 6.9 ‰ for $\alpha^{17}(CO_2/O_2)$ and $\alpha^{18}(CO_2/O_2)$, respectively; Table 2). If thermal diffusion is indeed responsible for the discrepancies between the theoretical equilibrium values and the experimental results, the offset is also expected to depend on the relative volumes of the cold and hot zones of the reactor. Indeed, at 750°C, Adnew et al[16] reported a slightly higher (thus closer to the theoretical value) value of $\alpha^{18}(CO_2/O_2)$, 1.000998 vs. 1.00051 (see Table 1), using a similar experimental setup except that in the previous study the volume of the cold zone of the reactor was smaller and without a stainless-steel extension (see Figure 1 and Figure S1, supporting information). As shown in Figure 6, the offset between theory and experiment depends on the temperature gradient between the hot and cold zones of the reactor. The cross-over temperature and the discrepancy between the theoretically calculated equilibrium and experimentally determined steady-state α values might depend on the geometry of the reactor, the pressure in of the reactor, the volume of the reactor, and the proportion of the cold and hot part of the reactor.

Oxygen three-isotope phenomena due to thermal diffusion have been investigated previously using pure gases[63,64] and the experiments indicate that fractionation effects are well established in static reactors exposed to spatial temperature gradients. Due to mass balance, fractionation effects in these studies disappeared when the temperature gradient was removed after the experiment and the system was allowed to equilibrate. This is different to our situation, where cooling the reactor to room temperature implies that the O_2-CO_2 exchange shuts down.

The fact that the experimental α values differ from theoretically equilibrium calculated data demonstrates that dynamical effects drive the system out of thermodynamic equilibrium. While kinetic isotope fractionation might occur in processes on the surface or at the solid–gas interface, the presence of a catalytic surface alone cannot change the thermodynamic equilibrium in the gas phase, by its very definition.[68] This implies that fractionation effects involving the catalytical substance are annihilated in forward and reverse reactions.[68] Similar to isotope fractionation in evaporation, surface chemical kinetics can only induce fractionation between O_2 and CO_2 if rapid removal processes in the gas phase prevent equilibrium being established.[69] The thermal gradient inducing a disequilibrium in the gas phase could possibly provide the required kinetic removal and thus potentially allow for surface kinetics to impact the O_2-CO_2 equilibration. However, without further quantitative analysis, such effects cannot be distinguished from the isotope fractionation due to thermal diffusion, which also come into play once a thermal gradient is established. Contrary to previous claims, surface-induced isotope

effects during O_2-CO_2 equilibration[25] cannot be studied without considering the impact of thermal diffusion.

4.3 | θ (CO_2/O_2) of the CO_2-O_2 isotope exchange

Experimentally determined θ (CO_2/O_2) values are larger than the canonical high temperature limit (θ >0.5305), an observation already made in previous studies.[12,19,70] Fosu et al[12] interpreted this as additional evidence that the CO_2-O_2 isotope exchange must be kinetically controlled. The experimentally determined θ (CO_2/O_2) takes extreme values when $^{18}\alpha$ (CO_2/O_2) is close to unity (near the crossover temperature where the sign of fractionation between CO_2 and O_2 changes, see Figure 7). These observations are a consequence of a singular behavior of θ close to the crossover, a well described anomaly in isotope equilibria.[32,71–75] Nevertheless, the experimentally determined θ values may not represent the CO_2-O_2 equilibrium exchange due to the possible thermal diffusion effect (see above) and other heterogenous process involving adsorption, desorption, and mixing.[12,19,28,29] As a result, the experimentally determined θ values are steady-state values.

It is interesting to investigate further the calculated θ (CO_2/O_2). Theoretically calculated values for $^{17}\alpha$ (CO_2/O_2) and $^{18}\alpha$ (CO_2/O_2) lead to values of $\theta = \ln(^{17}\alpha)/\ln(^{18}\alpha)$ which are outside the "canonical" range, i.e. θ > 0.5305 (see Figure 7). The upper bound of this conventional range arises from the high temperature limit (HTL) of the harmonic oscillator approximation (e.g. Young et al,[50] Cao and Liu,[31] Dauphas and Schauble,[53] Matsuhisa et al,[51] Kaiser et al[76]).

$$\theta_{\mathrm{HTL}} = \frac{m_{16}^{-1} - m_{17}^{-1}}{m_{16}^{-1} - m_{18}^{-1}} = 0.5305 \tag{5}$$

Examples in support of the approximation usually come from considering diatomic molecules, such as CO or O_2, for example (Cao and Liu,[31] Wang et al[54]). Here, we provide evidence that this empirical rule may not hold for more complex molecules like CO_2. The calculated temperature dependence of the three-isotope exponents for O + O_2 (θ_{O-O_2}) and O + CO_2 (θ_{O-CO_2}) isotope exchange reactions is shown in Figure S2 (supporting information). The three-isotope exponent for atom-molecule exchange (κ) is calculated as shown in Equation 6) following Cao and Liu.[31]

$$\theta_{\mathrm{O-XO}} = \kappa_{\mathrm{XO}} = \frac{\ln(^{17}\beta_{\mathrm{XO}})}{\ln(^{18}\beta_{\mathrm{XO}})} \tag{6}$$

where κ_{XO} or (θ_{O-XO}) is the three-isotope exponent for atom-molecule exchange, which should also be restricted to the parameter range < θ_{HTL}. This is indeed the case for O_2, but κ_{CO_2} clearly exceeds the expected range. According to our calculations, it reaches a HTL of around 0.533. We suppose that some structure in the results above 800°C is likely to be due to the smallness of the isotopic signatures, as well as to the precision and potential incompleteness of excited states in the line lists. While our κ_{O_2} value further agrees with the calculation of Cao and Liu,[31] to the fourth decimal place (or even better), our κ_{CO_2} value is higher by 0.0027 to 0.0035 over the full T range and it falls well above the canonical range, even at room temperature, where $\kappa_{CO_2}(25°C) = 0.5317$ (see Figure S2, supporting information).

Cao and Liu[31] have shown that the three-isotope exponent (θ_{a-b}) for isotope exchange between two molecules a and b can also be calculated as a linear combination of the three-isotope exponents κ_a and κ_b of the atom–molecule exchange equilibria for molecules a and b (see Equation 6), respectively:

$$\theta_{a-b} = (1-c)\,\kappa_a + c\,\kappa_b, \text{where } c = -\frac{\ln(^{18}\beta_b)}{\ln(^{18}\alpha_{a-b})} \tag{7}$$

Interestingly, the coefficient c in Equation 7 does not depend on ^{17}O, it only depends on ^{18}O via the $^{18}\beta$-value of molecule b and the (statistically corrected) equilibrium constant $^{18}\alpha_{a-b}$ between molecules a and b.

We can use this relationship and the well-studied H_2O-CO_2 system for an independent estimate of κ_{CO_2}. The three-isotope relationship between liquid water and gaseous CO_2 ($\theta_{CO_2-H_2O(l)}$) was experimentally determined to be 0.5229 at 25°C ($\alpha^{18}_{CO_2-H_2O(l)} = 1.041036$).[77] Using $\kappa_{H_2O} = 0.5300$ calculated for water vapor by Cao and Liu[31] (a similar κ_{H_2O} value was derived by the same authors from literature data on the gas vapor equilibrium) and $^{18}\beta_{CO_2} = 1.1194$ (this study), κ_{CO_2} can be calculated using Equation (7), yielding 0.5324 at 25°C. This also is clearly larger than the canonical HTL. The result is only slightly different (+0.0001) when $^{18}\beta_{CO_2} = 1.1171$ (from Richet et al[30]) is used, in contrast to $\kappa_{CO_2} = 0.5280$ as obtained by Cao and Liu.[31] As a cautionary note, it needs to be pointed out that the κ_{H_2O} value of Cao and Liu[31] was obtained without taking into account non-Born-Oppenheimer effects that seem to be important for water at room temperature.[57] When we use our value of $\kappa_{CO_2}(25°C) = 0.5317$ to determine $\kappa_{H_2O(l)}$ via Equation 7, from the measurements of $\alpha^{18}_{CO_2-H_2O(l)} = 1.041036$[77] and $\theta_{CO_2-H_2O(l)} = 0.5229$[77] and $^{18}\beta_{CO_2} = 1.1194$, we obtain $\kappa_{H_2O(l)} = 0.5294$. Interestingly, Barkan and Luz[78] have also determined the equilibrium fractionation factors between the gaseous and liquid phases of H_2O, from which the three-isotope coefficient $\theta_{CO_2-H_2O(g)} = 0.5241$ for the equilibrium fractionation of water and CO_2 in the gaseous phase can be derived. The corresponding $\alpha^{18}_{CO_2-H_2O(g)} = 1.05082$ implies that $\kappa_{H_2O(g)} = 0.5377$ using our $\kappa_{CO_2} = 0.5317$, or $\kappa_{H_2O(g)} = 0.5311$ when using the lower κ_{CO_2} from Cao and Liu.[31] Independently of the way of calculating κ_{CO_2}, available data on the CO_2-H_2O system seem to indicate that $\kappa_{H_2O(g)}$ also exceeds the canonical range limit. This implies that κ values of a chemical compound in different states might not be identical.

The independently derived κ_{CO_2} value of 0.5324 is somewhat higher than the value calculated directly from the experimentally improved ab-initio data from Huang et al,[42] $\kappa_{CO_2} = \ln\left(^{17}\beta_{CO_2}\right)/\ln\left(^{18}\beta_{CO_2}\right) = 0.5317$, and supports our finding that κ_{CO_2}(slightly) exceeds the value of 0.5305 even at room temperature. At high temperatures (~1000°C), κ_{CO_2} should be even higher, by 0.01 to 0.02. This is in striking contrast to the κ_{CO_2} values estimated by Cao and Liu[31] which never exceed 0.5305, but their underlying

calculations of partition function ratios seem to include only a limited number of anharmonic or higher order corrections to the simple harmonic oscillator approximation. Such corrections seem to be mostly negligible in the calculation of κ for diatomic molecules, such as O_2, for which the κ_{O_2} values calculated in this study (κ_{O_2} at 25°C = 0.5282, for example) are in perfect agreement with the values estimated by Cao and Liu.[31] Nevertheless, they appear to be important for triatomic molecules (H_2O, CO_2, etc.) and probably for more complex molecules too.

Finally, Equation 7 can be used to determine $\theta_{CO_2-O_2}$ independent of our evaluation of $^{17}\alpha$ (if it is suspected that the ^{17}O data are less reliable than the other data, for example) or even independent of $^{18}\alpha$. Using $\kappa_{CO_2}(25°C) = 0.5324$ (see previous paragraph), $\kappa_{O_2}(25°C) = 0.5282$, $^{18}\alpha = 1.0352$ (1.0372) and $^{18}\beta_{O2} = 1.0813$ (1.0773), results in $\theta_{CO_2-O_2} = 0.5419$ (0.5410). The values in parentheses are the corresponding values of Richet et al.[30] For comparison, the calculation based on the direct sum method for CO_2 used in this study yields $\theta_{CO_2-O_2} = 0.5396$ (0.5388) at 25°C, with the value in parentheses again being from the compilation of Richet et al.[30] Both routes of calculation yield values around 0.540, well beyond the "canonical range".

According to Equation 7, the combination of both the unusually large $\kappa_{CO_2} > 0.5305$ (exceeding κ_{O_2}) and the relatively large and opposite-sign coefficients of $c \simeq -2$ and $(1-c) \simeq 3$ leads to the exceptionally high value of $\theta_{CO_2-O_2} = 0.5396$. Nevertheless, the $O + CO_2$ exchange alone with $\kappa_{CO_2} \simeq 0.533$ at temperatures above 300°C must be regarded as the origin of this exception since standard values of κ_{CO_2} close to κ_{O_2} would not lead to such departures, regardless of the coefficient c in Equation (7). The solid theoretical and experimental evidence for $\kappa_{CO_2} > 0.5305$ and θ (CO_2/O_2) ~ 0.54 implies that analysis of three-isotope effects in CO_2 needs to go beyond the simple rigid-rotor harmonic oscillator analysis. This might also apply to other non-diatomic molecules and clumped isotope effects.[79] The above analysis of the CO_2-H_2O system seems to support this hypothesis concerning the oxygen isotopic fractionation of the H_2O molecule.

5 | CONCLUSIONS

The steady-state fractionation factors, $\alpha^{17}(CO_2/O_2)$ and $\alpha^{18}(CO_2/O_2)$, for the CO_2-O_2 isotope exchange reaction depend on temperature, largely explaining differences between previously reported values. Nevertheless, all our experimentally determined values are lower than those obtained from the updated theoretical calculations of equilibrium fractionation, and the offset is strictly mass-dependent. The discrepancy between the theoretical and experimental fractionation factors might be caused by thermal diffusion effects. While this requires further investigation, it provides an explanation for the inconsistent values reported in the literature.

We have shown that the CO_2-O_2 isotopic exchange under equilibrium conditions is characterized by unusual oxygen three-isotope behavior. Calculated θ (CO_2-O_2) values based on the direct sum method for CO_2, which includes anharmonic corrections, are larger than the canonical range limit for mass-dependent fractionation processes (0.5305), which possibly needs to be extended to 0.54. The result can be derived independently using the experimentally determined θ (CO_2/H_2O) and $\alpha^{18}(CO_2/H_2O)$ values, together with the theoretically calculated fractionation factor (β) for oxygen exchange between CO_2 and atomic O. Our analysis shows that the unusual behavior is linked to the energy levels of CO_2 isotopologues. This could imply the need for more accurate representation of energy terms (beyond the simple Bigeleisen-Mayer model) for poly-atomic molecules.

ACKNOWLEDGEMENTS

The authors thank Eugeni Barkan and Rolf Vieten from the Hebrew University of Jerusalem for calibration of their O_2 and CO_2 working gases. GAA is supported by EU Horizon 2020 ERC-ASICA project with a research grant number 64908 and project ALWPP.2016.013 of the Dutch Science Foundation NWO. The authors thank Wouter Peters from Wageningen University for collaboration and funding through ASICA. The authors appreciate the two anonymous reviewers for their constructive feedback which improved the manuscript.

PEER REVIEW

The peer review history for this article is available at https://publons.com/publon/10.1002/rcm.9301.

DATA AVAILABILITY STATEMENT

All the data used in this study are reported in the form of Figures and Tables.

ORCID

Getachew Agmuas Adnew https://orcid.org/0000-0002-1999-5664

Evelyn Workman https://orcid.org/0000-0002-7798-1690

REFERENCES

1. Adnew GA, Pons TL, Koren G, Peters W, Röckmann T. Leaf-scale quantification of the effect of photosynthetic gas exchange on $\Delta^{17}O$ of atmospheric CO_2. *Biogeosciences*. 2020;17(14):3903-3922. doi:10.5194/bg-17-3903-2020
2. Hofmann MEG, Horváth B, Schneider L, Peters W, Schützenmeister K, Pack A. Atmospheric measurements of $\Delta^{17}O$ in CO_2 in Göttingen, Germany reveal a seasonal cycle driven by biospheric uptake. *Geochim Cosmochim AC*. 2017;199:143-163. doi:10.1016/j.gca.2016.11.019
3. Liang M-C, Mahata S, Laskar AH, Thiemens MH, Newman S. Oxygen isotope anomaly in tropospheric CO_2 and implications for CO_2 residence time in the atmosphere and gross primary productivity. *Sci Rep*. 2017;7(1):13180 doi:10.1038/s41598-017-12774-w
4. Laskar AH, Mahata S, Liang M-C. Identification of anthropogenic CO_2 using triple oxygen and clumped isotopes. *Environ Sci Technol*. 2016;50(21):11806-11814. doi:10.1021/acs.est.6b02989
5. Hoag KJ, Still CJ, Fung IY, Boering KA. Triple oxygen isotope composition of tropospheric carbon dioxide as a tracer of terrestrial gross carbon fluxes. *Geophys Res Lett*. 2005;32(2):L02802 doi:10.1029/2004GL021011
6. Koren G, Schneider L, van der Velde IR, et al. Global 3-D simulations of the triple oxygen isotope signature $\Delta^{17}O$ in atmospheric CO_2.

J Geophys Res Atmos. 2019;124(15):8808-8836. doi:10.1029/2019JD030387
7. Luz B, Barkan E, Bender ML, Thiemens MK, Boering KA. Triple-isotope composition of atmospheric oxygen as a tracer of biosphere productivity. *Nature*. 1999;400(6744):547-550. doi:10.1038/22987
8. Thiemens MK, Chakraborty S, Jackson TL. Decadal $\Delta^{17}O$ record of tropospheric CO_2: Verification of a stratospheric component in the troposphere. *J Geophys Res Atmos*. 2014;119(10):6221-6229. doi:10.1002/2013JD020317
9. Landais A, Barkan E, Yakir D, Luz B. The triple isotopic composition of oxygen in leaf water. *Geochim Cosmochim ac*. 2006;70(16):4105-4115. doi:10.1016/j.gca.2006.06.1545
10. Landais A, Barkan E, Luz B. Record of $\delta^{18}O$ and ^{17}O-excess in ice from Vostok Antarctica during the last 150,000 years. *Geophys Res Lett*. 2008;35(2):L02709 doi:10.1029/2007GL032096
11. Sha L, Mahata S, Duan P, et al. A novel application of triple oxygen isotope ratios of speleothems. *Geochim Cosmochim Acta*. 2020;270:360-378. doi:10.1016/j.gca.2019.12.003
12. Fosu BJ, Subba R, Peethambaran R, Bhattacharya SK, Ghosh P. Developments and applications in triple oxygen isotope analysis of carbonates. *ACS Earth Space Chem*. 2020;4(5):702-710. doi:10.1021/acsearthspacechem.9b00330
13. Liljestrand F. The application of silica $\Delta^{17}O$ and $\delta^{18}O$ towards paleo-environmental reconstructions. Doctoral dissertation, Harvard University, Graduate School of Arts & Sciences. 2019.
14. Crockford PW, Hayles JA, Bao H, et al. Triple oxygen isotope evidence for limited mid-Proterozoic primary productivity. *Nature*. 2018;559(7715):613-616. doi:10.1038/s41586-018-0349-y
15. Thiemens MH. History and applications of mass-independent isotope effects. *Annu Rev Earth Planet Sci*. 2006;34(1):217-262. doi:10.1146/annurev.earth.34.031405.125026
16. Adnew GA, Hofmann MEG, Paul D, et al. Determination of the triple oxygen and carbon isotopic composition of CO_2 from atomic ion fragments formed in the ion source of the 253 Ultra high-resolution isotope ratio mass spectrometer. *Rapid Commun Mass Spectrom*. 2019;33(17):1363-1380. doi:10.1002/rcm.8478
17. Hofmann MEG, Pack A. Technique for high-precision analysis of triple oxygen isotope ratios in carbon dioxide. *Anal Chem*. 2010;82(11):4357-4361. doi:10.1021/ac902731m
18. Mahata S, Bhattacharya SK, Wang CH, Liang M-C. Oxygen isotope exchange between O_2 and CO_2 over hot platinum: An innovative technique for measuring $\Delta^{17}O$ in CO_2. *Anal Chem*. 2013;85(14):6894-6901. doi:10.1021/ac4011777
19. Barkan E, Musan I, Luz B. High-precision measurements of $\delta^{17}O$ and ^{17}O-excess of NBS19 and NBS18. *Rapid Commun Mass Spectrom*. 2015;29(23):2219-2224. doi:10.1002/rcm.7378
20. Affek HP, Barka E. A new method for high-precision measurements of $^{17}O/^{16}O$ ratios in H_2O. *Rapid Commun Mass Spectrom*. 2018;32(23):2096-2097. doi:10.1002/rcm.8290
21. Liang M-C, Mahata S. Oxygen anomaly in near surface carbon dioxide reveals deep stratospheric intrusion. *Sci Rep*. 2015;5(1):11352 doi:10.1038/srep11352
22. Laskar AM, Mahata S, Bhattacharya SK, Liang M-C. Triple oxygen and clumped isotope compositions of CO_2 in the middle troposphere. *Earth Space Sci*. 2019;6(1):1205-1219. doi:10.1029/2019EA000573
23. Laskar HA, Abhayanand SM, Vishvendra S, Bhola RG, Liang M-C. A new perspective of probing the level of pollution in the megacity Delhi affected by crop residue burning using the triple oxygen isotope technique in atmospheric CO_2. *Environ Pollut*. 2020;263(Pt A):114542 doi:10.1016/j.envpol.2020.114542
24. Daëron M, Blamart D, Peral M, Affek HP. Absolute isotopic abundance ratios and the accuracy of Δ_{47} measurements. *Chem Geol*. 2016;442:83-96. doi:10.1016/j.chemgeo.2016.08.014
25. Olack G, Colman AS. Modeling the measurement: Δ_{47}, corrections, and absolute ratios for reference materials. *Geochem Geophys Geosyst*. 2019;20(7):3569-3587. doi:10.1029/2018GC008166
26. Saenger CP, Schauer AJ, Heitmann OE, Huntington KW, Steig EJ. How ^{17}O excess in clumped isotope reference-frame materials and ETH standards affects reconstructed temperature. *Chem Geol*. 2021;563:120059 doi:10.1016/j.chemgeo.2021.120059
27. Adnew GA, Hofmann MEG, Pons TL, et al. Leaf scale quantification of the effect of photosynthetic gas exchange on Δ47 of CO2. *Sci Rep*. 2021;11:14023. doi:10.1038/s41598-021-93092-0
28. Mahata S, Bhattacharya SK, Liang MC. An improved method for high precision determination of $\Delta^{17}O$ by oxygen isotope exchange between O_2 and CO_2 over hot platinum. *Rapid Commun Mass Spectrom*. 2016;30(1):119-131. doi:10.1002/rcm.7423
29. Prasanna K, Bhattacharya SK, Ghosh P, Mahata S, Liang M-C. Isotopic homogenization and scrambling associated with oxygen isotopic exchange on hot platinum: Studies on gas pairs (O_2, CO_2) and (CO, CO_2). *RSC Adv*. 2016;6(56):51296-51303. doi:10.1039/C6RA08286F
30. Richet P, Bottinga Y, Javoy M. A review of hydrogen, carbon, nitrogen, oxygen, sulphur, and chlorine stable isotope fractionation among gaseous molecules. *Annu Rev Earth Planet Sci*. 1977;5(1):65-110. doi:10.1146/annurev.ea.05.050177.000433
31. Cao X, Liu Y. Equilibrium mass-dependent fractionation relationships for triple oxygen isotopes. *Geochim Cosmochim Acta*. 2011;75(23):7435-7445. doi:10.1016/j.gca.2011.09.048
32. Hayles JA, Cao X, Bao H. The statistical mechanical basis of the triple isotope fractionation relationship. *Geochem Perspect Lett*. 2017;3:1-11.
33. Schauble EA. Applying stable isotope fractionation theory to new systems. *Rev Mineral Geochem*. 2004;55(1):65-111. doi:10.2138/gsrmg.55.1.65
34. Urey HC. The thermodynamic properties of isotopic substances. *J Chem Soc*. 1947;562-581:562 doi:10.1039/jr9470000562
35. Bigeleisen J, Mayer MG. Calculation of equilibrium constants for isotopic exchange reactions. *J Chem Phys*. 1947;15(5):261-267. doi:10.1063/1.1746492
36. Dunham JL. The energy levels of a rotating vibrator. *Phys Ther Rev*. 1932;41(6):721-731. doi:10.1103/PhysRev.41.721
37. Huber KP, Herzberg G. *Molecular Spectra and Molecular Structure*. *Springer Science & Business Media*; 2013.
38. Wang M, Huang WJ, Kondev FG, Audi G, Naimi S. The AME 2020 atomic mass evaluation (II). Tables, graphs and references. *Chinese Phys C*. 2021;45(3):030003 doi:10.1088/1674-1137/abddaf
39. Irikura KK. Experimental vibrational zero-point energies: Diatomic molecules. *J Phys Chem*. 2007;36(2):389-397. doi:10.1063/1.2436891
40. Janssen C, Tuzson B. Isotope evidence for ozone formation on surfaces. *J Phys Chem*. 2010;A114:9709-9719.
41. Huang X, Gamache RR, Freedman RS, Schwenke DW, Lee TJ. Reliable infrared line lists for $^{13}CO_2$ isotopologues up to E'=18,000 cm^{-1} and 1500 K, with line shape parameters. *J Quant Spectrosc Radiat Transfer*. 2014;147:134-144.
42. Huang X, Schwenke DW, Freedman RS, Lee TJ. Ames-2016 line lists for 13 isotopologues of CO_2: Updates, consistency, and remaining issues. *J Quant Spectrosc Radiat Transfer*. 2017;203:224-241. doi:10.1016/j.jqsrt.2017.04.026
43. Prokhorov I, Kluge T, Janssen C. Optical clumped isotope thermometry of carbon dioxide. *Sci Rep*. 2019;9(1):4765 doi:10.1038/s41598-019-40750-z
44. Webb MA, Miller TF III. Position-specific and clumped stable isotope studies: Comparison of the Urey and path-integral approaches for carbon dioxide, nitrous oxide, methane, and propane. *J Phys Chem A*. 2014;118(2):467-474. doi:10.1021/jp411134v

45. Grebenshchikov SY. Photodissociation of carbon dioxide in singlet valence electronic states. I. Six multiply intersecting ab initio potential energy. *J Chem Phys*. 2013;138:224106
46. Barkan E, Luz B. Conversion of O_2 into CO_2 for high-precision oxygen isotope measurements. *Anal Chem*. 1996;68(19):3507-3510. doi:10.1021/ac9602938
47. Kroopnick P, Craig H. Oxygen isotope fractionation in dissolved oxygen in the deep sea. *Earth Planet Sci Lett*. 1976;32(2):375-388. doi:10.1016/0012-821X(76)90078-9
48. Taylor HP, Epstein S. Relationship between $^{18}O/^{16}O$ ratios in coexisting minerals of igneous and metamorphic rocks: Part 1: Principles and experimental results. *Geol Soc Am Bull*. 1962;73(4):461-480. doi:10.1130/0016-7606(1962)73[461:RBORIC]2.0.CO;2
49. Taylor HP. $^{18}O/^{16}O$ ratios in coexisting minerals of igneous and metamorphic rocks. PhD thesis, California Institute of Technology, Pasadena, CA, USA. 1959:40–43.
50. Young ED, Galy A, Nagahara H. Kinetic and equilibrium mass-dependent isotope fractionation laws in nature and their geochemical and cosmochemical significance. *Geochim Cosmochim AC*. 2002;66(6):1095-1104. doi:10.1016/S0016-7037(01)00832-8
51. Matsuhisa Y, Goldsmith JR, Clayton RN. Mechanisms of hydrothermal crystallization of quartz at 250°C and 15 kbar. *Geochim Cosmochim Acta*. 1978;42(2):173-182. doi:10.1016/0016-7037(78)90130-8
52. Weston RE. Anomalous or mass-independent isotope effects. *Chem Rev*. 1999;99(8):2115-2136. doi:10.1021/cr9800154
53. Dauphas N, Schauble EA. Mass fractionation laws, mass-independent effects, and isotopic anomalies. *Annu Rev Earth Planet Sci*. 2016;44(1):709-784. doi:10.1146/annurev-earth-060115-012157
54. Wang Z, Schauble EA, Eiler JM. Equilibrium thermodynamics of multiply substituted isotopologues of molecular gases. *Geochim Cosmochim Acta*. 2004;68(23):4779-4797. doi:10.1016/j.gca.2004.05.039
55. Gamache RR, Roller C, Lopes E, et al. Total internal partition sums for 166 isotopologues of 51 molecules important in planetary atmospheres: Application to HITRAN2016 and beyond. *J Quant Spectrosc Radiat Transfer*. 2017;203:70-87. doi:10.1016/j.jqsrt.2017.03.045
56. Born M, Huang K. *Dynamical Theory of Crystal Lattices*. International series of monographs on physics. Oxford: Clarendon Press; 1956.
57. Zhang Y, Liu Y. The theory of equilibrium isotope fractionations for gaseous molecules under super-cold conditions. *Geochim Cosmochim Acta*. 2018;238:123-149. doi:10.1016/j.gca.2018.07.001
58. Blatt H. Oxygen isotopes and the origin of quartz. *J Sediment Res*. 1987;57(2):373-377. doi:10.1306/212F8B34-2B24-11D7-8648000102C1865D
59. Abernathey JR, Rosenberger F. Soret diffusion and convective stability in a closed vertical cylinder. *Phys Fluids*. 1981;24(3):377 doi:10.1063/1.863381
60. Jones RC, Furry WH. The separation of isotopes by thermal diffusion. *Rev Mod Phys*. 1946;18(2):151-223. doi:10.1103/RevModPhys.18.151
61. Ageev EP, Panchenkov GM. The separation of oxygen isotopes by thermal diffusion. *Soviet Atomic Energy*. 1964;14(5):518-520. doi:10.1007/BF01121902
62. Müller G, Vasaru G. The Clusius-Dickel thermal diffusion column – 50 years after its invention. *Isotopenpraxis*. 1988;24(11-12):455-464. doi:10.1080/10256018808624027
63. Sun T, Bao H. Thermal-gradient-induced non-mass-dependent isotope fractionation. *Rapid Commun Mass Spectrom*. 2011;25(6):765-773. doi:10.1002/rcm.4912
64. Sun T, Bao H. Non-mass-dependent ^{17}O anomalies generated by a superimposed thermal gradient on a rarefied O_2 gas in a closed system. *Rapid Commun Mass Spectrom*. 2011;25(1):20-24. doi:10.1002/rcm.4825
65. Hirschfelder OJ, Curtiss CF, Bird RB. *Molecular theory of gases and liquids*. New York: John Wiley and Sons, Inc.; 1964.
66. Olson JM, Rosenberger F. Convective instabilities in a closed vertical cylinder heated from below. Part 2. Binary gas mixtures. *J Fluid Mech*. 1979;92(4):609-629. doi:10.1017/S0022112079000781
67. Anav A, Friedlingstein P, Beer C, et al. Spatiotemporal patterns of terrestrial gross primary production: A review. *Rev Geophys*. 2015;53(3):785-818. doi:10.1002/2015RG000483
68. Laidler KJ, Meiser JH, Sanctuary BC. *Physical Chemistry*. Houghton Mifflin; 2002.
69. Mook W. *Environmental isotopes in the hydrological cycle: principles and applications*. Vol. 1. International Atomic Energy Agency and United Nations Educational, Scientific and Cultural Organization; 2000:39.
70. Passey BH, Levin NE. Triple oxygen isotopes in meteoric waters, carbonates, and biological apatites: Implications for continental paleoclimate reconstruction. *Rev Mineral Geochem*. 2021;86(1):429-462. doi:10.2138/rmg.2021.86.13
71. Kotaka M, Okamoto M, Bigeleisen J. Anomalous mass effects in isotopic exchange equilibria. *J Am Chem Soc*. 1992;114(16):6436-6445. doi:10.1021/ja00042a022
72. Deines P. A note on intra-elemental isotope effects and the interpretation of non-mass-dependent isotope variations. *Chem Geol*. 2003;199(1-2):179-182. doi:10.1016/S0009-2541(03)00076-7
73. Otake T, Lasaga AC, Ohmoto H. Ab initio calculations for equilibrium fractionations in multiple sulfur isotope systems. *Chem Geol*. 2008;249(3-4):357-376. doi:10.1016/j.chemgeo.2008.01.020
74. Spindel W, Stern MJ, Monse EU. Further studies on temperature dependences of isotope effects. *J Chem Phys*. 1970;52(4):2022-2035. doi:10.1063/1.1673255
75. Vogel PC, Stern MJ. Temperature dependences of kinetic isotope effects. *J Chem Phys*. 1971;54(2):779-796. doi:10.1063/1.1674912
76. Kaiser J, Röckmann T, Brenninkmeijer CAM. Contribution of mass-dependent fractionation to the oxygen isotope anomaly of atmospheric nitrous oxide. *J Geophys Res*. 2004;109:D03305
77. Barkan E, Luz B. High-precision measurements of $^{17}O/^{16}O$ and $^{18}O/^{16}O$ ratios in CO_2. *Rapid Commun Mass Spectrom*. 2012;26(23):2733-2738. doi:10.1002/rcm.6400
78. Barkan E, Luz B. High precision measurements of $^{17}O/^{16}O$ and $^{18}O/^{16}O$ ratios in H_2O. *Rapid Commun Mass Spectrom*. 2005;19(24):3737-3742. doi:10.1002/rcm.2250
79. Liu Q, Tossell JA, Liu Y. On the proper use of the Bigeleisen–Mayer equation and corrections to it in the calculation of isotopic fractionation equilibrium constants. *Geochim Cosmochim Acta*. 2010;74(24):6965-6983. doi:10.1016/j.gca.2010.09.014

SUPPORTING INFORMATION

Additional supporting information may be found in the online version of the article at the publisher's website.

How to cite this article: Adnew GA, Workman E, Janssen C, Röckmann T. Temperature dependence of isotopic fractionation in the CO_2-O_2 isotope exchange reaction. *Rapid Commun Mass Spectrom*. 2022;36(12):e9301. doi:10.1002/rcm.9301